Rare Met.
DOI 10.1007/s12598-014-0382-4

RARE METALS
www.editorialmanager.com/rmet

Performance of $Sm_{0.7}Sr_{0.3}CoO_{3-\delta}$ membrane under CO_2-containing atmosphere

Yu-Wen Zhang*, Fan-Lin Zeng, Chen-Chen Yu, Cheng-Zhang Wu, Wei-Zhong Ding, Xiong-Gang Lu

Received: 15 November 2013 / Revised: 2 December 2013 / Accepted: 18 August 2014
© The Nonferrous Metals Society of China and Springer-Verlag Berlin Heidelberg 2014

Abstract The permeability and stability of $Sm_{0.7}Sr_{0.3}CoO_{3-\delta}$ (SSCO) regarding the special requirements for carbon capture and storage (CCS) application were investigated. Pure CO_2 was used as the sweep gas at 900 °C, leading to that the oxygen permeation flux decreases by about 34 %. Several cycles of changing the sweep gas between helium and CO_2 indicate the good reversibility of this degradation. Both carbonate formation and adsorption of CO_2 on the membrane surface are responsible for the degradation of the membrane performance. The better CO_2 resistance results from the substitution of Sm for Sr due to the higher acidity of Sm_2O_3 (1.278) than that of SrO (0.978) and a discontinuous layer of carbonate.

Keywords $Sm_{0.7}Sr_{0.3}CoO_{3-\delta}$; Oxygen permeation; CO_2; Carbonate; Perovskite

1 Introduction

Power generation from fossil fuel results in serious environmental problems because of the emission of large amount of CO_2. Integrating dense mixed ion–electron conducting (MIEC) membranes into power cycles with CO_2 capture is considered as the most advanced technology for high efficiency and clean power production [1–4]. However, the operation environment of MIEC membranes in the fuel combustion with pure oxygen (oxy-fuel process) is harsh and the main requirements are CO_2 tolerance and high permeability.

It is a great challenge for the highly permeable perovskite membranes which usually contain amounts of basic elements such as alkaline earth metals, and thus readily react with the acidic CO_2. For instance, when $Ba(Co_{0.4}Fe_{0.6-x}Zr_x)O_{3-\delta}$ [5], $Ba_{0.5}Sr_{0.5}Co_{0.8}Fe_{0.2}O_{3-\delta}$ [6, 7], and $BaCo_{0.7}Fe_{0.2}Nb_{0.1}O_{3-\delta}$ [8, 9] were exposed to CO_2, an instant cessation of the oxygen permeation was observed within a few minutes. A compact and continuous layer of carbonate was proposed to be responsible for the degradation of the membrane performance. To improve the performance of perovskite materials, cation substitution is an effective method. Recent studies suggest co-doping with high valence metal elements in B-site, such as Nb [9], Ti [10, 11], and Ta [12], which posses high stabilized energies, in order to improve the stability under CO_2 atmosphere. Compared with the alteration of B-site cations, the substitution of A-site cations is also a good choice because they tend to react with CO_2 directly. Recent studies showed that by partial substituting Sr^{2+} at the A-site in $SrCoO_{3-\delta}$ with Sm^{3+}, $Sm_xSr_{1-x}CoO_{3-\delta}$ membrane possesses excellent permeability and preserves good stability [13–16]. The $Sm_{0.6}Sr_{0.4}CoO_{3-\delta}$ material was first reported as MIEC membrane by Teraoka et al. [17]. As for $Sm_xSr_{1-x}CoO_{3-\delta}$, the highest conductivity of around 500 $S \cdot cm^{-1}$ at 1,000 °C was obtained for $Sm_{0.7}Sr_{0.3}CoO_{3-\delta}$ [18]. Although a few information is already available, the detailed examination of $Sm_{0.7}Sr_{0.3}CoO_{3-\delta}$ (SSCO) regarding the special requirements for oxy-fuel process is still lacking. Therefore, the oxygen permeation and stability of $Sm_{0.7}Sr_{0.3}CoO_{3-\delta}$ perovskite regarding oxy-fuel process were investigated under CO_2-containing atmosphere in this paper.

Y.-W. Zhang*, F.-L. Zeng, C.-C. Yu, C.-Z. Wu, W.-Z. Ding, X.-G. Lu
Shanghai Key Laboratory of Modern Metallurgy and Materials Processing, Shanghai University, Shanghai 200072, China
e-mail: springzyw@shu.edu.cn

Published online: 05 October 2014

2 Experimental

2.1 Synthesis and preparation

The $Sm_{0.7}Sr_{0.3}CoO_{3-\delta}$ powder was prepared through the solid state reaction. The required stoichiometry of Sm_2O_3, $SrCO_3$, and Co_2O_3 was milled in ethanol using zirconia grinding media for 60 h in a planetary ball-miller, and the powder was calcined at 950 °C for 20 h. The calcined powder was ball milled in ethanol for 24 h. Ceramic samples were compressed by a uniaxial single-acting press at 50 MPa into discoid membranes and sintered at 1,150 and 1,200 °C, respectively, in ambient air for 5–10 h. The final diameter of the membranes was 16 mm and the thickness was 1 mm. The densities of the sintered membranes were determined by gas pycnometer (Micrometritics AccuPycII1340). Only membranes with relative densities higher than 90 % were used for experiments.

2.2 Oxygen permeation

Permeation properties of the discoid membranes under different atmospheres were investigated by gas chromatography (GC, VARIAN CP-3800) method using a vertical high-temperature oxygen permeation apparatus [19]. A discoid membrane was sealed to the reactor with a silver seal. The effective inner surface area and the thickness of the discoid membranes were controlled around 1.3 cm^2 and 1 mm, respectively. The gas flow rates were controlled by mass flow controllers (MFC). The flow rate of experimental gas was calibrated by a soap-film flow-meter. The operating temperature was controlled by the thermocouple near the membranes.

2.3 Characterization

The behaviors of SSCO samples in N_2 + 10 % CO_2 and CO_2 atmosphere were characterized by thermogravimetry (TG, Netzsch, STA449C). The phase and crystal structures of the sintered membranes and the samples after experiments were characterized by X-ray diffractometer (XRD, Rigaku D-Max/RB). The changes of the morphology of the membranes were analyzed by scanning electron microscope (SEM, JEOL JSM-6700F). Their compositions after reaction were determined by energy dispersive X-ray spectroscopy (EDX, OXFORD INCA).

3 Results and discussion

3.1 Permeability of SSCO under gradient of CO_2/air

The influence of different CO_2 contents in the sweep gas on the permeation flux of SSCO membrane at 900 °C is shown in Fig. 1. Initially, the sweep gas consists of pure helium before switching to a mixture of CO_2 and helium (10 % and 100 % CO_2 content). The total sweep flow rate was kept constant at 100 $cm^3 \cdot min^{-1}$ and the air with a flow rate of 110 $cm^3 \cdot min^{-1}$ was used as feed gas. If helium is used as sweep gas, a constant permeation flux of 0.56 $cm^3 \cdot cm^{-2} \cdot min^{-1}$ is obtained. After switching to sweep gas consisting of helium and CO_2, a decrease of the permeation flux as a function of time and CO_2 content is observed. At 10 % CO_2, the permeation flux decreases by about 21 %, but finally a constant permeation flux of 0.44 $cm^3 \cdot cm^{-2} \cdot min^{-1}$ is achieved. If the CO_2 content on the sweep side increases further to 100 %, the decrease of the oxygen permeation flux is accelerated with a higher CO_2 content. At 100 % CO_2, 34 % lower permeation flux is observed. If the sweep gas is shifted back to 10 % CO_2, the oxygen permeation flux of about 0.4 $cm^3 \cdot cm^{-2} \cdot min^{-1}$ is obtained again.

Figure 2 presents the oxygen permeation flux through the SSCO membrane when the sweep gas periodically changes between helium and CO_2 at 900 °C. When using

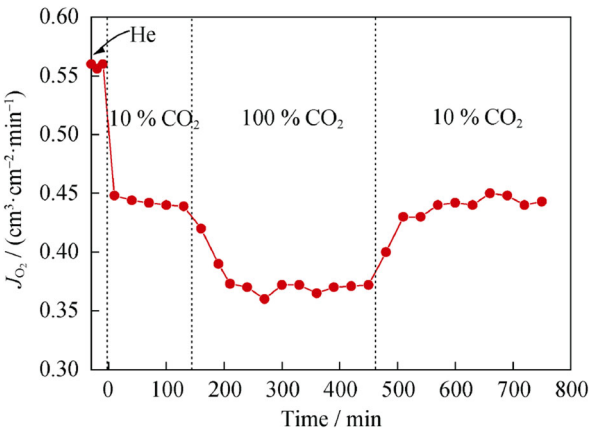

Fig. 1 Effect of CO_2 concentration in sweep gas on oxygen permeation flux

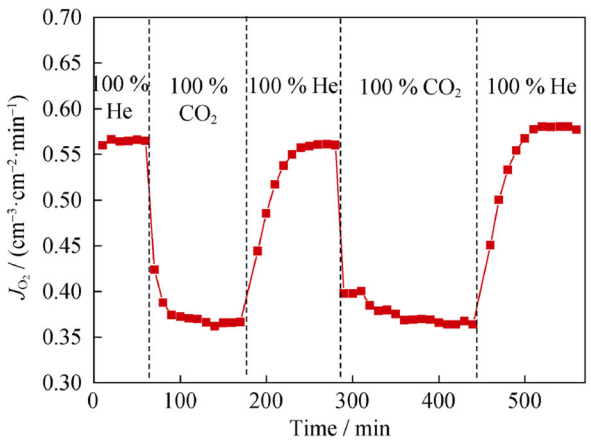

Fig. 2 Oxygen permeation flux with sweep gas changing

helium as sweep gas, a stable oxygen permeation flux of 0.56 $cm^3 \cdot cm^{-1} \cdot min^{-1}$ can be obtained, whereas the oxygen permeation flux decreases immediately to a lower value of 0.37 $cm^3 \cdot cm^{-1} \cdot min^{-1}$ if CO_2 instead of helium was used as sweep gas. However, if the sweep gas is shifted back to pure helium, the original oxygen permeation flux is obtained. The similar reversibility is found for other oxygen-permeable membranes when the sweep gas changes between CO_2 and inert gas [6–9].

Figure 3 shows absorption curves of SSCO in (N_2 + 10 % CO_2) and CO_2 atmospheres obtained by TG analysis. The heating rate is 10 °C·min^{-1}. In both atmospheres, the weight of SSCO samples changes gradually with the increase of temperature in a similar trend. The initial loss happens and the weight starts to increase rapidly around 700 °C and decreases at above 900 °C. The decrease of weight at above 700 °C is due to the oxygen loss. The considerable increase of the weight of the sample above this temperature is caused by the absorption of CO_2 and the formation of carbonate. The drop at higher temperature is due to the decomposition accompanied by the revolution of CO_2. The beginning temperatures for the decomposition of carbonate under 10 % CO_2 and 100 % CO_2 are about 914 and 945 °C, respectively. This behavior is well-known from studies on related materials [20, 21].

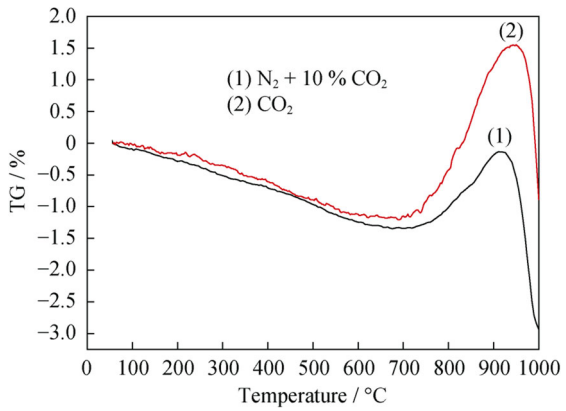

Fig. 3 Thermal gravimetric graphs of SSCO in different atmospheres

3.2 Microstructure change of SSCO under different conditions

SEM images of the fresh and used SSCO membranes are presented in Fig. 4 and the EDX analyses for the designated areas in Fig. 4 are given in Table 1.The used sample is the one after the experiment of the influence of different CO_2 contents in the sweep gas on the permeation flux. The surface of the fresh SSCO membrane shows the individual grains (Fig. 4a). It can be seen from Fig. 4b and c that a reaction zone is observed on the surface of the SSCO membrane surface which is in contact with CO_2. The secondary phase with small size is observed, which grows to form a new layer covering the sample surface. The newly formed surface layer consists mainly of Sm, Sr, Co, C, and O, as shown in the designated areas in Fig. 4b and c and presented in Table 1. Therefore, the new surface layer can be ascribed to a mixture of carbonates and mixed-oxides. This is further confirmed by XRD analysis in Fig. 5.

After the experiment of the influence of different CO_2 contents in the sweep gas on the permeation flux, the surface of the used SSCO sample was characterized by XRD, as presented in Fig. 5. It can be seen that the fresh membrane shows the perovskite structure and can be indexed in an orthorhombic and trigonal symmetry. The phases observed in the present study are similar to previous report [17]. And XRD analysis for the surface exposed to CO_2 shows carbonate phases which are found to be strontium carbonate ($SrCO_3$). The additional phases $Sr_2Co_2O_5$, Sm_2O_3, and CoO are also observed for the used sample. The results are consistent with the EDS analysis (Table 1).

Table 1 EDS reuslts of designated area in Fig. 4 (at%)

Areas	Sm	Sr	Co	O	C
1	1.9	10.8	1.6	19.5	66.2
2	7.2	16.8	7.0	45.5	23.5

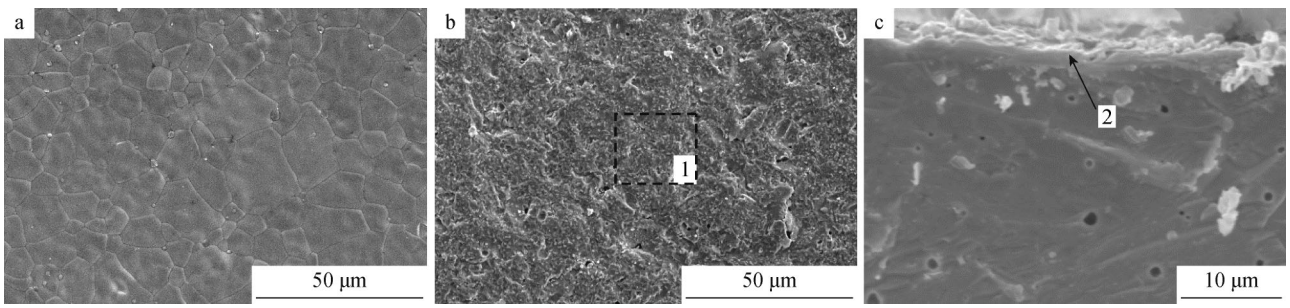

Fig. 4 SEM images of fresh and used SSCO membranes: **a** surface of fresh membrane, **b** surface of used membrane, and **c** cross section of used membrane

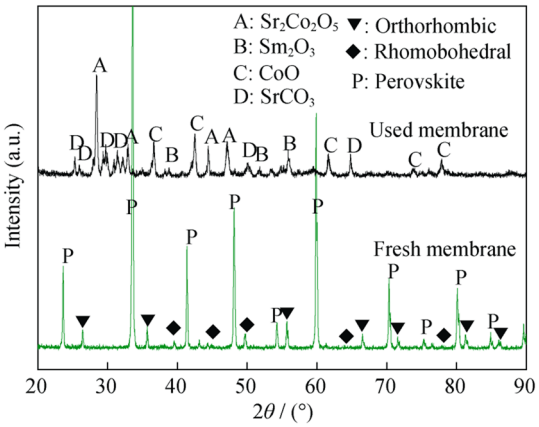

Fig. 5 XRD patterns of fresh and used SSCO membranes

When CO_2 is introduced into the sweep gas, the oxygen permeation flux of SSCO decreases immediately to a lower value. The layer of carbonate forming on the membrane surfaces is proposed to be responsible for the degradation of the membrane performance [5–9]. According to the SEM and XRD analysis of the used SSCO membrane exposed to CO_2, the microstructures of the surface and the cross section near the permeated side show the typical form of a carbonate phase (Figs. 4, 5). The carbonate layer could hinder the oxygen permeation. However, this cannot explain the increase of the permeation flux when the concentration of CO_2 in the sweep gas decreases from 100 % to 10 %. When the concentration of CO_2 decreases from 100 % to 10 %, the carbonate on the membrane surface under 100 % CO_2 cannot decompose under the mixture of 10 % CO_2 according to the thermodynamic data (HSC Chemistry, ESM Software 5.1, 2005). As shown in Fig. 3, the formed carbonate begins to decompose under 10 % CO_2 at above 914 °C. There must be other reasons for the change of the permeation flux under different concentrations of CO_2. Previous studies showed that CO_2 can be strongly absorbed on the surface of pervoskite oxides and hinder the oxygen surface exchange process [22, 23]. The initial flux reduction of SSCO after changing helium to CO_2 may be due to the adsorption of CO_2 on the membrane surface, resulting in a slower oxygen surface exchange rate. Under different concentrations of CO_2, there is a different equilibrium between the adsorption and desorption of CO_2 on the SSCO surface. The higher the concentration of CO_2 in sweep gas is, the more the CO_2 is adsorbed on the SSCO membrane surface. As a result, the oxygen surface exchange rate decreases significantly, and the different oxygen permeation fluxes are obtained under the mixture of CO_2 with different concentrations though the formed carbonate cannot decompose.

After a long-term operation under CO_2, the content of Sr increases on the permeation side (Table 1). This indicates that the growth of the carbonate layer is a diffusion-controlled process and $SrCO_3$ grows outward at the outer surface of the membrane. This mechanism is in good agreement with that for other oxygen-permeable membranes [6]. The following mechanism may be assumed for the structural degradation of SSCO in CO_2. Firstly, part of Sr^{2+} leaves the SSCO perovskite; concurrently, $Sr_2Co_2O_5$, Sm_2O_3, and CoO form. Subsequently, Sr^{2+} diffuses through the perovskite product phase in the decomposed zone to the gas–solid interface; simultaneously, co-current transport of the electrons takes place. Sr^{2+} reacts with CO_2 and oxygen ions at the outer solid surface, resulting in the growth of the $SrCO_3$ layer. In a general form, the overall reaction is

$$Sm_{0.7}Sr_{0.3}CoO_{3-\delta} + CO_2 \rightarrow SrCO_3 + Sr_2Co_2O_5 + Sm_2O_3 + CoO \quad (1)$$

As shown in Fig. 2, when the CO_2 sweep gas is shifted to helium, the oxygen permeation flux of SSCO is totally recovered. It might be assumed that the recovery of the permeation flux is accompanied by the reconstruction of the phases on the membrane surfaces and the oxygen vacancies in lattice. This presumption on the phase reconstruction on the membrane surfaces is proven by XRD analysis. At the end of flux recovery experiments, the membrane was cooled in a helium atmosphere after the sweep gas was switched from CO_2 to helium. The sweep and feed sides of the experimental membrane were characterized by XRD, as presented in Fig. 6. For comparison, the XRD pattern of the original membrane is also listed in Fig. 6. The extra reflection peaks that exist in the fresh membrane decrease and the perovskite phases are observed. No reflection peaks that are ascribed to carbonates are observed, indicating the decomposition of the $SrCO_3$ surface layer which blocks the membrane surface. However, the original perovskite phase and dense grain structure are not regenerated thoroughly. Yi et al. [9] reported that the oxygen permeability of $BaCo_{1-x-y}$

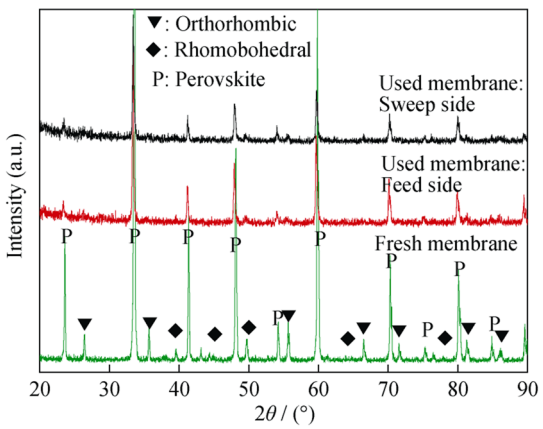

Fig. 6 XRD patterns of fresh and sweep and free sides of used SSCO membranes

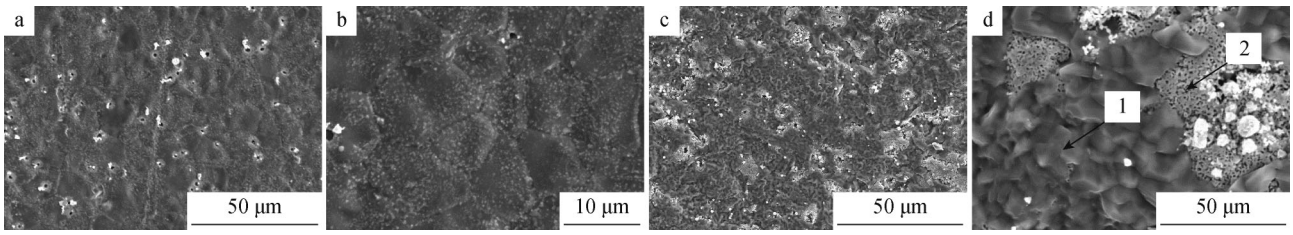

Fig. 7 SEM image of SSCO membrane surface annealed in CO_2 at 900 °C for **a**, **b** 2 h and **c**, **d** 100 h. **b** and **d** being magnifications of **a** and **c**, respectively

$Fe_xNb_yO_{3-\delta}$ degraded by CO_2 can be largely recovered by a CO_2-free inert gas and the $BaCo_xO_y$ phase surface layer instead of the original $BaCo_{1-x-y}Fe_xNb_yO_{3-\delta}$ perovskite phase were observed. They also found that neither the parent perovskite phase nor the dense grain structure present in the as-prepared sample was regenerated after Ar recovery. With the sweep gas changing from CO_2 to helium and the decomposition of the formed carbonate, the desorption of CO_2 from the membrane surface happens and the oxygen vacancies in lattice also reconstruct. When an equilibrium of desorption and adsorption of CO_2 on the membrane surfaces reaches, a stable permeation flux recovers gradually.

It is noteworthy that SSCO membrane can retain a high oxygen permeation flux when exposed to pure CO_2. This behavior is different to previous findings on the perovskite-type membranes. Arnold et al. [6] observed an instant cessation of the oxygen permeation for $Ba_{0.5}Sr_{0.5}Co_{0.8}Fe_{0.2}O_{3-\delta}$ membrane, when the membrane was subjected to a pure CO_2 sweep gas at 875 °C. A rapid breakdown of the oxygen permeability through (Ba, Sr)(Zn, Fe)$O_{3-\delta}$ membrane at 750 °C in CO_2 atmosphere was reported [24]. Upon switching the sweep gas from the CO_2-free inert gas to pure CO_2, the oxygen flux of $BaCo_{0.7}Fe_{0.2}Nb_{0.1}O_{3-\delta}$ and $BaCo_{0.6}Fe_{0.2}Nb_{0.2}O_{3-\delta}$ decreases to an undetectable level almost instantly at 800–1,000 °C [8, 9]. A compact and continuous layer of carbonate on the surface of the membrane exposed to CO_2 is proposed to be responsible for the breakdown of the membrane performance. However, the permeation flux decreasing by only 34 % is observed for SSCO when exposed to pure CO_2. The good CO_2 resistance of SSCO benefits from the substitution of the A-site cation. The $ABO_{3-\delta}$ perovskite usually contains a significant amount of alkaline earth elements on the A-site which exhibit high basicity, and thus it readily reacts with the acidic CO_2. Generally, the reactivity of metal oxide with acidic gas, CO_2, can be reflected by (Lewis) acidity, leaving alone other effects (e.g., structure and stoichiometry). Higher acidity of the metal oxide corresponds to better resistance to CO_2. The acidities of Sm_2O_3 and SrO are 1.278 and 0.978, respectively [25]. The better CO_2 resistance of SSCO resulting from partial substitution of Sm for Sr is consistent with the higher acidity of Sm_2O_3 compared with that of SrO.

Table 2 EDS results of designated area in Fig. 7d (at%)

Areas	Sm	Sr	Co	O	C
1	1.6	13.3	1.4	20.1	63.6
2	34.5	2.5	14.2	41.8	7.0

When SSCO membrane is exposed to CO_2, the A-site Sr readily reacts with CO_2 to form $SrCO_3$ (Figs. 4, 5). The atom ratio of Sm to Sr in SSCO is 7/3, and it is difficult to form a continuous layer of carbonate $SrCO_3$ on the membrane surface. This is confirmed by another experiment. In order to better understand the surface structure of SSCO exposed to CO_2, pellet samples were annealed in pure CO_2 at 900 °C for 2 and 100 h. SEM images of the annealed SSCO are presented in Fig. 7 and the EDS analysis on the designated areas in Fig. 7d is given in Table 2. After exposure to CO_2 for 2 h, the secondary phase with small size is observed (Fig. 7a, b), which grows to form a layer of carbonate after 100 h (Fig. 7c, d and Table 2). But the layers of carbonate do not cover the membrane surface thoroughly. Though the layer of carbonate could hinder the oxygen permeation, the uncovered area on the membrane surface could supply the channel for the oxygen permeation. This also contributes to the high oxygen permeation flux of SSCO when exposed to pure CO_2. For $BaCo_{0.6}Fe_{0.2}Nb_{0.2}O_{3-\delta}$, significant $BaCO_3$ formation is already found after being annealed in CO_2 shortly for 3 min, and a compact and continuous layer of carbonate grows quickly [9]. So, the permeation flux of $BaCo_{0.6}Fe_{0.2}Nb_{0.2}O_{3-\delta}$ drops almost instantaneously to a negligible level when switching the sweep gas from Ar to CO_2 at 900 °C.

4 Conclusion

Both the oxygen permeability and the microstructure of SSCO membranes were investigated under the condition of CO_2. Using pure CO_2 as sweep gas causes the permeation flux to decrease by about 34 %, but it can be easily recovered by sweeping with pure helium. Reaction of the SSCO membrane with CO_2 leads to the decomposition of the membrane surface and the formation of a mixture of

$SrCO_3$ and mixed-oxides, such as $Sr_2Co_2O_5$, Sm_2O_3, and CoO. The enrichment of strontium at the sweep side indicates that the growth of the carbonate layer is a diffusion-controlled process, and $SrCO_3$ grows outward at the outer surface of the membrane. The substitution of Sm for Sr in the perovskite leads to the improvement of CO_2 resistance, which may be attributed to the increase of the oxide acidity and the discontinuous layer of carbonate.

Acknowledgments This work was financially supported by the National Natural Science Foundation of China (Nos. 51174133, 51274139 and 51225401) and the Science and Technology Commission of Shanghai Municipality (No.11ZR1412900). The authors would like to thank Yu-Liang Chu for SEM analysis work.

References

[1] Habib MA, Nemitallah M, Ben-Mansour R. Recent development in oxy-combustion technology and its applications to gas turbine combustors and ITM reactors. Energy Fuels. 2013;27(1):2.

[2] Engels S, Beggel F, Modigell M, Stadler H. Simulation of a membrane unit for oxyfuel power plants under consideration of realistic BSCF membrane properties. J Membr Sci. 2010;359(1–2):93.

[3] Ben-Mansour R, Habib MA, Badr H. Characteristics of oxy-fuel combustion in an oxygen transport reactor. Energy Fuels. 2012;26(7):4599.

[4] Leo A, Liu SM, João C, Diniz da Costa. Development of mixed conducting membranes for clean coal energy delivery. Int J Greenhouse Gas Control. 2009;3(4):357.

[5] Tong JH, Yang WS, Zhu BC, Cai R. Investigation of ideal zirconium-doped perovskite-type ceramic membrane materials for oxygen separation. J Membr Sci. 2002;203(1–2):175.

[6] Arnold M, Wang HH, Feldhoff A. Influence of CO_2 on the oxygen permeation performance and the microstructure of perovskite-type $(Ba_{0.5}Sr_{0.5})(Co_{0.8}Fe_{0.2})O_{3-\delta}$ membranes. J Membr Sci. 2007;293(1–2):44.

[7] Engels S, Markus T, Modigell M, Singheiser L. Oxygen permeation and stability investigations on MIEC membrane materials under operating conditions for power plant processes. J Membr Sci. 2011;370(1):58.

[8] Yi JX, Schroeder M, Weirich T, Mayer J. Behavior of Ba(Co, Fe, Bb)$O_{3-\delta}$ perovskite in CO_2-containing atmosphere: degradation mechanism and materials design. Chem Mater. 2010; 22(23):6246.

[9] Yi JX, Weirich TE, Schroeder M. CO_2 corrosion and recovery of perovskite-type $BaCo_{1-x-y}Fe_xNb_yO_{3-\delta}$ membranes. J Membr Sci. 2013;437(15):49.

[10] Schulz M, Kriegel R, Kämpfer A. Assessment of CO_2 stability and oxygen flux of oxygen permeable membranes. J Membr Sci. 2011;378(1–2):10.

[11] Zeng Q, Zuo YB, Fan CG, Chen CS. CO_2-tolerant oxygen separation membranes targeting CO_2 capture application. J Membr Sci. 2009;335(1–2):140.

[12] Zuo JH, Yue M, Lu QM, Zhang DT, Gao XX, Zhang JX, Guo ZH, Li W. Structure, magnetic properties, and thermal stability of $Sm_{1-x}Tm_xCo_5$ compounds. Rare Met. 2014;33(2):176.

[13] Gao M, Li CJ, Li CX, Yang GJ, Fan SQ. Microstructure, oxygen stoichiometry and electrical conductivity of flame-sprayed $Sm_{0.7}Sr_{0.3}CoO_{3-\delta}$. J Power Sources. 2009;191(2):275.

[14] Yang L, Zuo CD, Wang SZ, Cheng Z, Liu ML. A novel composite cathode for low-temperature SOFCs based on oxide proton conductors. Adv Mater. 2008;20(17):3280.

[15] Li XC, Zhang XY, Lu YJ, Li K. Interface reaction mechanism of welding Al_2O_3 ceramic with AgCuInTi brazing filler. Chin J Rare Met. 2013;37(1):71.

[16] Lv H, Wu YJ, Huang B, Zhao BY, Hu KA. Structure and electrochemical properties of $Sm_{0.5}Sr_{0.5}Co_{1-x}Fe_xO_{3-\delta}$ cathodes for solid oxide fuel cells. Solid State Ionics. 2006;177(9–10):901.

[17] Teraoka Y, Nobunaga T, Yamazoe N. Effect of cation substitution on the oxygen semipermeability of perovskite-type oxides. Chem Lett. 1988;3(4):503.

[18] Tu HY, Takeda Y, Imanishi N, Yamamoto O. $Ln_{1-x}Sr_xCoO_3$ (Ln = Sm, Dy) for the electrode of solid oxide fuel cells. Solid State Ionics. 1997;100(3–4):283.

[19] Zhang YW, Li Q, Shen PJ, Liu Y, Yang ZB, Ding WZ, Lu XG. Hydrogen amplification of coke oven gas by reforming of methane in a ceramic membrane reactor. Int J Hydrogen Energy. 2008;33(13):3311.

[20] Zhang WJ, Dai JM, Zhu XB, Chang Q, Liu QC, Sun YP. Improvement of dielectric tunability and loss tangent of (Ba, Sr)TiO_3 thin films with K doping. Chin Phys B. 2012;21(9):097702.

[21] Li YH, Zhang W, Dong C. Makino, Akihiro, Effects of Cu, Fe and Co addition on the glass-forming ability and mechanical properties of Zr–Al–Ni bulk metallic glasses. Sci China-Phys Mech Astron. 2012;55(12):2367.

[22] Pena M, Fierro J. Chemical structure and performance of perovskite oxides. Chem Rev. 2011;101(7):1981.

[23] Zhao Z, Liu L, Zhang XM, Wu WM, Tu BF, Ou DR, Cheng MJ. A comparison on effects of CO_2 on $La_{0.8}Sr_{0.2}MnO_{3+\delta}$ and $La_{0.6}Sr_{0.4}CoO_{3-\delta}$ cathodes. J Power Sources. 2013;222(15):542.

[24] Martynczuk J, Efimov K, Robben L, Feldhoff A. Performance of zinc-doped perovskite-type membranes at intermediate temperatures for long-term oxygen permeation and under a carbon dioxide atmosphere. J Membr Sci. 2009;344(1–2):62.

[25] Jeong NC, Lee JS, Tae EL, Lee YJ, Yoon KB. Acidity scale for metal oxides and Sanderson's electronegativities of lanthanide elements. Angew Chem Int Ed. 2008;47(52):10128.